

Growth kinetics of boride layers formed on 99.0% purity nickel

I GUNES^{1,*}, M KEDDAM², R CHEGROUNE² and M OZCATAL¹

¹Department of Metallurgical and Materials Engineering, Faculty of Technology, Afyon Kocatepe University, 03200 Afyonkarahisar, Turkey

²Laboratory of Materials Technology, Faculty of Mechanical Engineering and Process Engineering, USTHB, B.P. No. 32, 16111 El-Alia, Bab-Ezzouar, Algiers, Algeria

MS received 8 May 2014; accepted 3 February 2015

Abstract. The present study reports on the kinetics of borided Nickel 201 alloy. The thermochemical treatment of boronizing was carried out in a solid medium consisting of B₄C and KBF₄ powders mixture at 1123, 1173 and 1223 K for 2, 4 and 6 h, respectively. The boride layer was characterized by optical microscopy, X-ray diffraction technique and micro-Vickers hardness tester. X-ray diffraction analysis revealed the existence of NiB, Ni₂B, Ni₃B and Ni₄B₃ compounds at the surface of borided Nickel 201 alloy. The thickness of the boride layer increased with an increase in the boriding time and the temperature. The hardness of the nickel borides formed on the surface of the nickel substrate ranged from 1642 to 1854 HV_{0.05}, whereas the Vickers hardness value of the untreated nickel was 185 HV_{0.05}. The growth kinetics of boride layers forming on the borided Nickel 201 alloy was also analysed. The boron activation energy (Q) was estimated as equal to 203.87 kJ mol⁻¹ for the borided Nickel 201 alloy.

Keywords. Nickel 201 alloy; boride layer; micro-hardness; kinetics; activation energy.

1. Introduction

Boriding is a diffusional surface treatment, which is defined as an enrichment of the surface of a workpiece with boron. Main advantages of this technique lead to high strength of abrasion wear, corrosion and high oxidation resistance compared with other conventional surface treatments.^{1–3} The boriding treatment can be applied to a variety of metals, including ferrous and non-ferrous alloys: niobium, nickel, cobalt alloys and most refractory alloys.^{4–13} The boronizing process is a prominent choice for a wide range of tribological applications where the control of friction and wear is of primary concern.^{14–18} The boriding process involves heating the material in the temperature range of 973–1273 K during 1–12 h, in contact with a boronaceous solid powder, paste, liquid, gaseous, plasma, plasma paste and fluidized bed boriding. Boron atoms, because of their relatively small size (atomic radius of 0.9 Å) can easily diffuse into the substrate material (atomic radius of 1.24 Å) to form a hard boride layer.^{19–22} The boride layer thickness is influenced by alloying elements in the metal substrate (Cr, V and Mo) which can modify the active boron flux by entering the iron boride lattice. The amounts of C, Cr and Mo appear to be lower than that of iron in the boride layer because of less solubility. Thus, the deficiency of C, Cr and Mo results in a negative effect on the boride layer in terms of both thickness and morphology.^{23–25} Chromium and molybdenum

preferentially enter the coatings by substituting for iron in the FeB and Fe₂B phases. Carbon, which is insoluble in iron borides, concentrates strongly at the (boride layer/substrate) interface.^{2,26}

Ni and Ni-base alloys are used in various industrial plants and equipment for their high resistance to corrosion. Despite this superior property, its utilization fields are limited since it has a low hardness and weak wear performance. For this reason, it is necessary to improve their wear and corrosion resistance through surface hardening treatments.²⁵

In this study, the Nickel 201 alloy was borided considering these advantages of boriding. Characterization and growth kinetics of the obtained boride layers were studied.

The main objective of this study was to investigate the diffusion kinetics of borided Nickel 201 alloys in the temperature range of 1123–1223 K for variable exposure times (2, 4 and 6 h). In addition, the effect of boriding parameters on the properties of boride layers was also investigated.

2. Experimental

2.1 Boriding and characterization

Table 1 gives the chemical composition of the untreated Nickel 201 alloy. The samples had a cubic shape with dimensions of 10 × 10 × 10 mm³ and polished progressively with 1000-grit emery paper before the boronizing process. The boriding treatment was carried out in solid medium containing a B₄C and KBF₄ powder mixture placed in an electrical resistance furnace operated at temperatures of

*Author for correspondence (igunes@aku.edu.tr)

Table 1. The chemical composition of Nickel 201 alloy as a substrate (wt%).

Steels	Ni	C	Co	Fe	Mg	Mn	Si	Ti
Nickel 201	0.99	0.02	0.25	0.13	0.15	0.30	0.15	0.1

1123, 1173 and 1223 K for 2, 4 and 6 h, respectively, under atmospheric pressure. The microstructures of polished and etched cross-sections of the specimens were observed under a Nikon MA100 optical microscope. The thickness of borides was measured by means of a digital thickness measuring instrument attached to an optical microscope (Nikon MA100). The boride layer thickness values given in the results section are averages of at least 12 measurements. The contour diagram, showing the variation in boride layer thickness with respect to the boriding temperature and time, were plotted using the Sigma plot 12.5 program. The presence of borides formed in the coating layer was confirmed by means of X-ray diffraction (XRD) equipment (Shimadzu XRD 6000) using $\text{CuK}\alpha$ radiation. The hardness measurements of the boride layer on each borided and unborided Nickel 201 alloy substrate were made on the cross-sections using a Shimadzu HMV-2 Vickers indenter with a 50 g load.

2.2 Evaluation of the boron activation energy

In order to study the diffusion mechanism, borided Nickel 201 alloy was used for this purpose. It is assumed that the boride layers grow parabolically in the direction of diffusion flux and perpendicular to the substrate surface. Hence, the time dependence of boride layer thickness can be described as display

$$x^2 = Dt, \quad (1)$$

where x is the depth of the boride layer (μm), t the boriding time (s), D the boron diffusion coefficient through the boride layer. It is a well-known fact that the main factor limiting the growth of a layer is the diffusion of boron into the substrate.²⁷ Hence, the relationship between growth rate constant, D , activation energy, Q , and the temperature in Kelvin, T , can be expressed by the Arrhenius equation (equation (2)) as follows:

$$D = D_0 \exp\left(-\frac{Q}{RT}\right), \quad (2)$$

where D_0 is a pre-exponential constant, Q the activation energy (J mol^{-1}), T the absolute temperature in Kelvin and R is the ideal gas constant ($= 8.314 \text{ J mol}^{-1} \text{ K}^{-1}$).

The boron activation energy in the boride layer is determined by the slope obtained when plotting $\ln D$ vs. $1/T$, using

$$\ln D = \ln D_0 - \frac{Q}{RT}. \quad (3)$$

3. Results and discussion

3.1 Characterization of boride coatings

The cross-sections of optical micrographs of the borided Nickel 201 alloy at temperatures of 1123, 1173 and 1223 K for 6 h are shown in figure 1a–c. It is seen that the formed

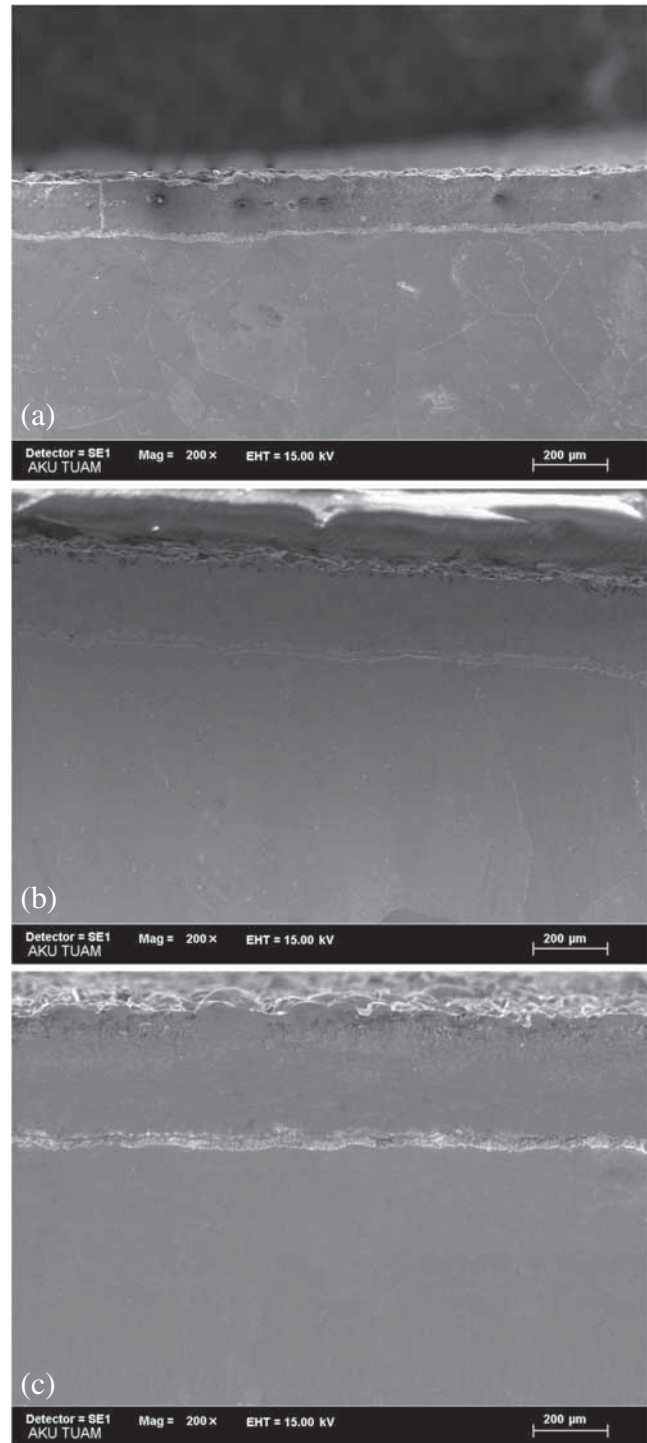


Figure 1. Cross-sections of the borided Nickel 201 alloy (a) 1123 K–6 h, (b) 1173 K–6 h and (c) 1223 K–6 h.

boride layers on the borided Nickel 201 alloy appear to be compact and regular and having a smooth interface.

Depending on the boriding parameters (time and temperature) the boride layer thickness on the surface of borided Nickel 201 alloy ranged from 39.62 and 312.58 μm as shown in figure 2. Figure 3a–d gives the XRD patterns recorded at the surface of boride Nickel 201 alloy at the two temperatures 1123 and 1223 K for 2 and 6 h, respectively.

XRD patterns indicated that the boride layers were composed of nickel borides (Ni_xB_y). The XRD results showed

that the boride layers formed on the Nickel 201 alloy, contained the NiB , Ni_2B , Ni_3B and Ni_4B_3 phases. The boride layers mainly consisting of intermetallic phases (Ni_xB_y) are resulting from the diffusion of boron atoms into the nickel substrate for the given boriding parameters. Ozbek *et al.*²⁸ have borided 99.5% purity nickel with Ekabor 2 boron powder at 1173–1223 K for 2–6 h and have shown the formation of Ni_5Si_2 and Ni_2B boride phases. Aytekin and Akcin²⁹ have also borided Incoloy 825 alloy with Ekabor 2 boron powder at 1223 K for 2–8 h and have obtained the NiB , Ni_2B , CrB , Cr_2B , FeB and Fe_2B phases.

Microhardness measurements were done from the surface to the interior along a line to see the variation of hardness through the boride layer. The microhardness of the boride layers was measured at 12 different locations at the same distance from the surface and an average value was taken as the hardness. Microhardness measurements were carried out on the cross-sections from the surface to the interior along a line. Figure 4 provides the microhardness profiles obtained at the surface of borided samples at 1123 and 1223 K for 2 and 6 h, respectively. Depending on the boriding temperature and time, the hardness of the boride layer formed on the Nickel 201 alloy varied between 1642 and 1854 $\text{HV}_{0.05}$, whereas the Vickers hardness value of the untreated Nickel 201 alloy was 186 $\text{HV}_{0.05}$. It is concluded that the boride layer hardness is approximately ten times greater than that of the nickel substrate. Mu *et al.*⁶ have borided pure nickel

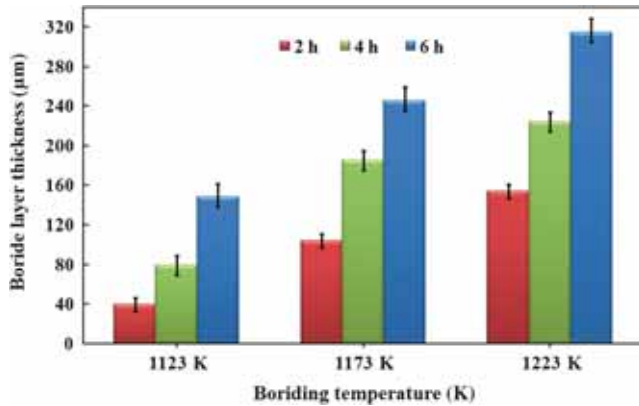


Figure 2. Thickness values of boride layers as a function of boriding parameters (time and temperature).

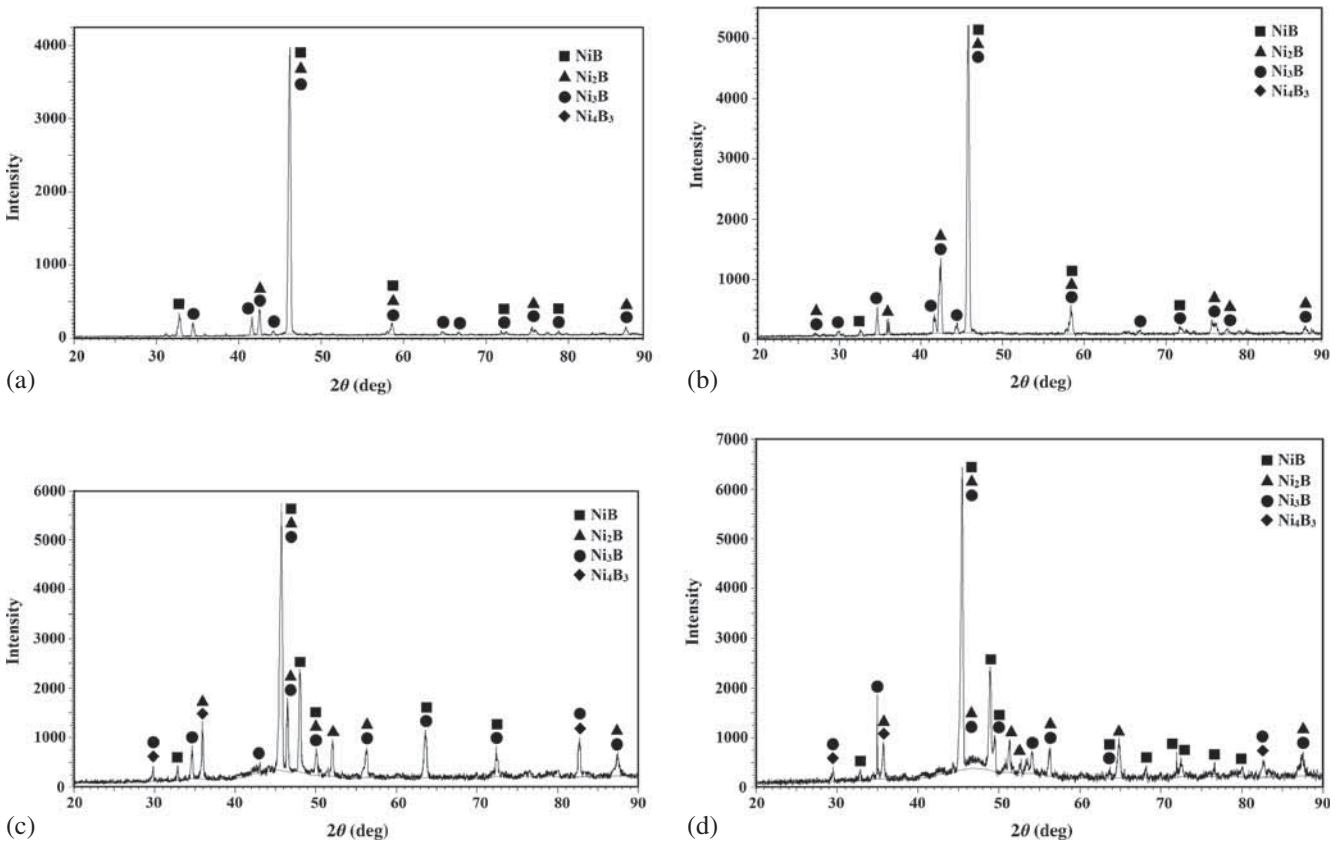


Figure 3. X-ray diffraction patterns of borided Nickel 201 alloy (a) 1123 K–2 h, (b) 1123 K–6 h, (c) 1223 K–2 h and (d) 1223 K–6 h.

using the mixture powders with SiC as diluent and have obtained a hardness value varying between 217 and 984 HV. Ozbek *et al*²⁸ have borided 99.5% purity nickel with Ekabor 2 boron powder at 1173–1223 K for 2–6 h and have obtained a hardness value located between 747 and 805 HV. A hardness value of 1300 HK was also found by Ueda *et al*²² when boriding the nickel substrate by the powder-pack method in the temperature range of 973–1173 K for 2–6 h. Lou *et al*⁷ have investigated the microstructure and properties of paste borided pure nickel and Nimonic 90 superalloy. In their experimental study, Nimonic 90 superalloy and pure nickel were successfully borided at 900, 950, 1000 and 1050°C for 2 and 5 h. The surface microhardness values of the two materials were significantly improved after boronizing (from 100 to 1100 HV_{0.1}) for borided nickel) and (between 400 and 2500 HV_{0.1}) for borided Nimonic 90 superalloy. Aytekin and Akcin²⁹ have treated the Incoloy 825 alloy with Ekabor 2 boron powder at 1223 K during 2–8 h and have obtained a hardness value changing between 690 and 1810 HV_{0.05}.

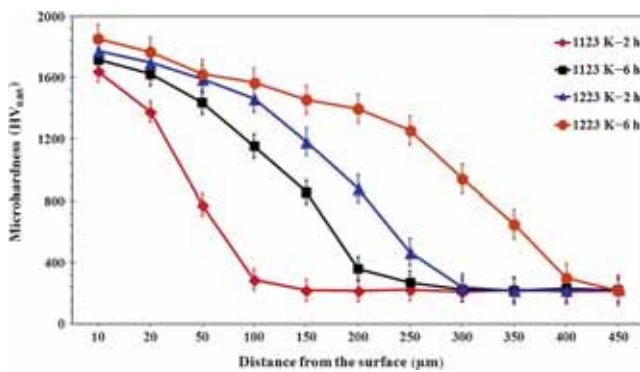


Figure 4. Microhardness profiles obtained at the surface of borided Nickel 201 alloy.

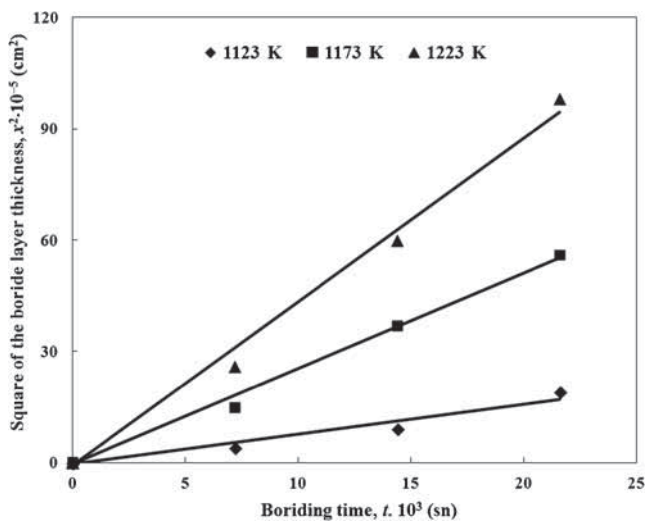


Figure 5. Time dependence of the square of boride layer thickness at increasing temperatures.

3.2 Kinetics

In this study, the effects of the boriding parameters on the growth kinetics of the boride layer were also investigated. Kinetic parameters such as processing temperature and time must be known for the control of the boriding treatment. Figure 5 shows the time dependence of the squared value of boride layer thickness at increasing temperatures. This evolution followed a parabolic growth law where the diffusion of boron atoms is a thermally activated phenomenon. The growth rate constant D at each boriding temperature can be easily calculated from equation (1).

As a result, the calculated growth rate constants at the three temperatures: 1123, 1173 and 1223 K are the following: 567×10^{-9} , 1774×10^{-9} and $5543 \times 10^{-9} \text{ cm}^2 \text{ s}^{-1}$ for the borided Nickel 201 alloy.

Figure 6 describes the temperature dependence of the growth rate constant. The plot of $\ln D$ as a function of the reciprocal temperature exhibits a linear relationship according to the Arrhenius equation. The boron activation energy can be easily obtained from the slope of the straight line presented in figure 6. The value of boron activation energy was then determined as equal to $203.87 \text{ kJ mol}^{-1}$ for the borided Nickel 201 alloy.

Table 2 compares the obtained value of boron activation energy ($20387 \text{ kJ mol}^{-1}$) with the data found in the literature. The calculated value in this study was compared with the values reported in the literature,^{19,30–33} as displayed in table 2. It is seen that the reported values of boron activation energy depended on the chemical composition of the substrate and on the boriding method used.

A contour diagram describing the evolution of boride layer thickness as a function of the boriding parameters (time and temperature) is shown in figure 7. This contour diagram can be used as a simple tool to predict the boride layer thickness on the basis of equation (1) for a given temperature and exposure time.³³ The boride layer increased with the increase in boriding time and temperature for the borided Nickel 201 alloy.

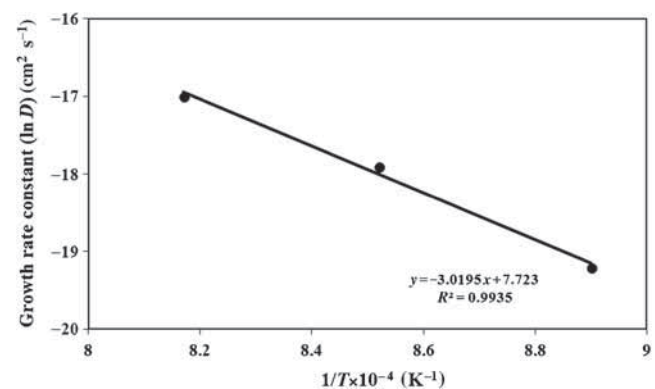
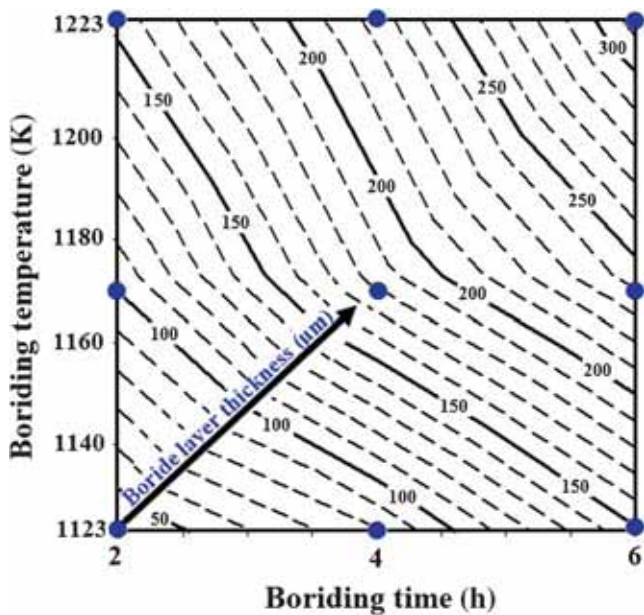


Figure 6. Temperature dependence of the growth rate constant according to the Arrhenius equation.

Table 2. Comparison of the boron activation energy for some materials depending on the boriding method.

Substrate	Temperature range (K)	Boriding medium	Activation energy (kJ mol ⁻¹)	References
Fe–Mn	1073–1373	Powder	119	19
Molybdenum	1273–1673	Spark plasma sintering	218.8	30
Pure iron	1223–1323	Paste	151	31
Ni ₃ Al	1123–1223	Powder	188	32
Ni ₃ Al	973–1073	Electrochemical	185.95	33
Nickel 201 alloy	1123–1223	Powder	203.87	Present study

**Figure 7.** Contour diagram describing the evolution of boride layer thickness as a function of boriding parameters (time and temperature).

4. Conclusions

The following conclusions may be derived from the present study:

- The boride layer formed on the surface of Nickel 201 alloy has a smooth and flat morphology.
- The multiphase boride coatings that were thermochemically grown on the Nickel 201 alloy were composed of NiB, Ni₂B, Ni₃B and Ni₄B₃ phases.
- Depending on the boriding parameters, the boride layer thickness obtained on the borided Nickel 201 alloy was ranged from 39.62 to 312.58 μm .
- Depending on the boriding temperature and time, the hardness of the boride layer formed on the Nickel 201 alloy varied between 1642 and 1854 HV_{0.05}, whereas Vickers hardness value of the untreated Nickel 201 alloy was 186 HV_{0.05}.
- As a result of boriding, the low surface hardness of the Nickel 201 alloy was improved.

- The boron activation energy was estimated as 20387 kJ mol⁻¹ for the borided Nickel 201 alloy.
- A contour diagram relating the boride layer thickness to the boriding parameters (time and temperature) was proposed. It can be used a simple tool to select the optimum boride layer thickness according to the practical utilization of this kind of material.

References

1. Genel K 2006 *Vacuum* **80** 451
2. Uslu I, Comert H, Ipek M, Ozdemir O and Bindal C 2007 *Mater. Des.* **28** 55
3. Gunes I 2014 *Mater. Technol.* **48** 765
4. Ribeiro R, Ingole S, Usta M, Bindal C, Ucisik A H and Liang H 2006 *Vacuum* **80** 1341
5. Keddarn M 2009 *Int. J. Mater. Res.* **100** 901
6. Mu D, Shen B, Yang C and Zhao X 2009 *Vacuum* **83** 1481
7. Lou D C, Solberg J K, Akselsen O M and Dahl N 2009 *Mater. Chem. Phys.* **115** 239
8. Anthymidis K G, Zinoviadis P, Roussos D and Tsipas D N 2002 *Mater. Res. Bull.* **37** 515
9. Mu D, Yang C, Shen B and Jiang H 2009 *J. Alloys Compd.* **479** 629
10. Usta M, Ozbek I, Bindal C, Ucisik A H, Ingole S and Liang H 2006 *Vacuum* **80** 1321
11. Campos-Silva I, Bravo-Bárceñas D, Meneses-Amador A, Ortiz-Dominguez M, Cimenoglu H, Figueroa-López U and Andraca-Adame J 2013 *Surf. Coat. Technol.* **237** 402
12. Usta M 2005 *Surf. Coat. Technol.* **194** 251
13. Usta M, Ozbek I, Ipek M, Bindal C and Ucisik A H 2005 *Surf. Coat. Technol.* **194** 330
14. Von Matuschka A G 1980 *Boronizing* (Philadelphia: Heyden and Son Inc.)
15. Bindal C and Ucisik A H 1999 *Surf. Coat. Technol.* **122** 208
16. Keddarn M 2004 *Appl. Surf. Sci.* **236** 451
17. Sen S, Sen U and Bindal C 2005 *Surf. Coat. Technol.* **191** 274
18. Ozbek I and Bindal C 2011 *Vacuum* **86** 391
19. Bektas M, Calik A, Ucar N and Keddarn M 2010 *Mater. Charact.* **61** 233
20. Ulker S, Gunes I and Taktak S 2011 *Indian J. Eng. Mater. Sci.* **18** 370
21. Gunes I, Ulker S and Taktak S 2011 *Mater. Des.* **32** 2380

22. Ueda N, Mizukoshi T, Demizu K, Sone T, Ikenaga A and Kawamoto M 2000 *Surf. Coat. Technol.* **126** 25
23. Sinha A K 1991 *J. Heat Treat.* **4** 437
24. Campos I, Ramirez G, Figueroa U, Martinez J and Morales O 2007 *Appl. Surf. Sci.* **253** 3469
25. Gunes I 2013 *Sadhana* **38** 527
26. Taktak S and Tasgetiren S 2006 *J. Mater. Eng. Perform.* **15** 570
27. Brakman C M, Gommers A W J and Mittemeijer E J 1989 *J. Mater. Res.* **4** 1354
28. Ozbek I, Akbulut H, Zeytin S, Bindal C and Ucisik A H 2000 *Surf. Coat. Technol.* **126** 166
29. Aytekin H and Akcin Y 2013 *Mater. Des.* **50** 515
30. Yu L G, Khor K A and Sundararajan G 2006 *Surf. Coat. Technol.* **201** 2849
31. Campos I, Oseguera J, Figueroa U, Garcı J A, Bautista O and Kelemenis G 2003 *Mater. Sci. Eng. A* **352** 261
32. Torun O 2008 *Surf. Coat. Technol.* **202** 3549
33. Kahvecioglu O, Sista V, Eryilmaz O L, Erdemir A and Timur S 2011 *Thin Solid Films* **520** 1575